

AFFDL-TR-72-5

**A TECHNIQUE FOR MEASURING
IN-PLANE DISPLACEMENTS BY
HOLOGRAPHIC INTERFEROMETRY**

*FRANK D. ADAMS
RICHARD R. CORWIN*

Approved for public release; distribution unlimited.

FOREWORD

This report was prepared by Dr. Frank D. Adams, of the Analysis Group, Solid Mechanics Branch, Structures Division, Air Force Flight Dynamics Laboratory (AFFDL/FBR), and Mr. Richard R. Corwin of Beta Industries, Inc., Dayton, Ohio. The work was conducted in-house under Project 1467, "Structural Analysis Methods", Task 146702, "Thermoelastic Analysis Methods". Mr. R. M. Bader (AFFDL/FBR) is the Technical Manager of the Analysis Group.

This report covers work conducted from January 1971 to September 1971. This report was submitted by the authors in January 1972.

This technical report has been reviewed and is approved.



FRANCIS J. JANIK, JR.
Chief, Solid Mechanics Branch
Structures Division
Air Force Flight Dynamics Laboratory

AFFDL-TR-72-5

ABSTRACT

An experimental technique for measuring in-plane displacements from a single hologram is described. The method is based upon imaging the entire wave reflected from a single point and recorded on a hologram. Experimental results are presented. Application and limitations of the technique are discussed.

TABLE OF CONTENTS

<u>SECTION</u>		<u>PAGE</u>
I	INTRODUCTION	1
II	MEASURING DISPLACEMENTS USING HOLOGRAPHIC INTERFEROMETRY	2
1.	Theoretical Review	2
2.	Techniques for Fringe Interpretation	4
3.	Accuracy and Minimum Detectability of In-Plane and Normal Components	6
a.	Accuracy and Minimum Detectable Limit of the Normal Component	7
b.	Accuracy and Minimum Detectable Limit of the In-Plane Component	8
c.	Summary	11
III	MEASUREMENT OF IN-PLANE DISPLACEMENTS USING LARGE APERTURE OBSERVATION	12
1.	Description of Technique	12
2.	Experimental Results	15
3.	Summary	20
IV	SUMMARY AND RECOMMENDATIONS	21
	REFERENCES	22

LIST OF ILLUSTRATIONS

<u>FIGURE</u>		<u>PAGE</u>
1.	Error in the In-Plane Component Assuming Visual Observation and a Hologram Aperture of 3.5 Inches	9
2.	Minimum Detectable In-Plane Component Assuming Visual Observation and a Hologram Aperture of 3.5 Inches	10
3.	Coordinate System for Observing the Diffracted Waves from an Object Point	13
4.	Optical System for Recording Fringe Shift Across Hologram Aperture	14
5.	System for Recording and Viewing Hologram	16
6.	Photograph of Image of the Translating Stage	17
7.	Photograph of Hologram Image of the Fringes	17
8.	Fringe Pattern from Single Object Point (4" Aperture)	19
9.	Fringe Pattern from Single Object Point (2 3/4" Aperture)	19

Contrails

LIST OF TABLES

<u>TABLE</u>		<u>PAGE</u>
1.	Comparison Between In-Plane and Normal Components Assuming a 3.5-Inch Aperture Located 35 Inches from the Object	11

SECTION I

INTRODUCTION

Much of the work in holographic interferometry has involved the measurement of components of displacement which are essentially normal to the hologram. An extensive amount of work has been accomplished in the measurement of amplitudes of vibrating plates and static deflections of beams which are normal to the hologram. Much less work has been accomplished in the measurement of in-plane components. Since holography is a three-dimensional imaging process, the capability exists for measuring both in-plane and normal displacements from a single hologram.

This report describes a technique for measuring in-plane displacements from a single hologram. The measurement technique is based upon imaging the entire wave reflected from a single object point and recorded on a hologram. In Section II the underlying theory is reviewed, and the measurement error and minimum detectable normal and in-plane components are derived in terms of the total available information recorded on a hologram. In Section III the underlying theory is reviewed, and the measurement error and minimum detectable normal and in-plane components are derived in terms of the total available information recorded on a double exposure hologram. In Section III preliminary experimental results are presented, and the potential applications and limitations of the technique are discussed.

SECTION II

MEASURING DISPLACEMENTS USING HOLOGRAPHIC INTERFEROMETRY

1. Theoretical Review

A hologram is a recording on a photographic plate of the interference between the light wave scattered by an object and a reference wave. When a hologram has been exposed, developed, and irradiated by a reconstruction wave with the same propagation direction as the original reference wave, a wave is produced which is an exact replica of the original wave scattered by the object. The scattered wave is characterized by an electric field which is a function of the illumination wave and the position of the scattering point.

There are two types of hologram interferometry, real-time and time-average. In real-time holography, a hologram of the object is first recorded and the resulting hologram image is made to coincide with the object by replacing the hologram back in its original recording position. If the object is made to undergo a time dependent motion, then a time varying fringe pattern can be observed in real-time. In time-average holography, an object is made to undergo some time-dependent motion and a hologram of the moving object is recorded for an interval of time, T. The resulting hologram image is an image of the stationary object and a fringe pattern. If all points on the object surface move with the same time function, then the fringe function can be written as (Ref. 1):

$$M(\Omega) = \frac{1}{T} \int_0^T \exp[i\Omega(\bar{R}, \bar{k}_s) f(t)] dt \quad (1)$$

where Ω is the argument function that describes the changes in amplitude,

Contrails

propagation direction, and phase of the plane wave components of the object field spectrum, $f(t)$ is the displacement-time function of the object, \bar{R} is a vector from the point on the object to the point in space where the fringe system is localized, and \bar{k} is the propagation vector of the wave scattered from the object point. For static displacements and double exposure holograms $f(t)$ takes on values of ± 1 and the fringe function is a cosine function, and for sinusoidal vibration of the object the fringe function will be a Bessel function (Ref. 2). The condition for fringe loci will be

$$M(\Omega) = 0 \quad (2)$$

That is, this condition will define the dark bands of the interference pattern. The bright bands will be given by the maxima of the fringe function.

The argument of Equations 1 and 2, the scalar phase change, is due to the movement of the object. For small displacements the scalar phase change is, in general, the sum of two effects (Ref. 1), a change in the bulk phase and a change in the propagation direction. This total scalar phase change has been formulated (Ref. 1, 3, 4) and is given by:

$$\Omega = \bar{L} \cdot (\bar{k}_2 - \bar{k}_1) - (\bar{R} - \bar{R}_0) \cdot \Delta \bar{k}_2 \quad (3)$$

where

\bar{L} = the total displacement vector at the object point whose position vector is \bar{R}_0 ,

\bar{k}_1 = the propagation vector of the incident wave at the object point,

\bar{k}_2 = the propagation vector of the reflected wave at the object point,

Contrails

\bar{R} = the position vector of the point in space imaged by the observation system, and

$\Delta \bar{k}_2$ = the change in the propagation direction of the reflected wave.

Those points in space in which the interference pattern can be observed with maximum visibility are commonly called the points of fringe localization. These points can be determined from the condition (Ref. 1, 4) that the partial derivatives of the scalar phase change with respect to the coordinates perpendicular to the axis of observation must go to zero. In Equation 3, the second term is identically zero; however, the partial derivatives of this term are not necessarily zero. Therefore, to compute fringe localization the second term must be retained, but to compute fringe loci the second term can be eliminated, to give the more familiar equation for phase change.

2. Techniques for Fringe Interpretation

This more complete form for the phase change relates to the additional information available in holographic interferometry. The scalar phase change is different for every point in space, and it is different for every ray that passes through a given point in space. In practice, the observing optical system is the human eye or a camera which is made to image on a localized fringe pattern. Further, the iris is small so that only a small bundle of rays passing through a given image point are selected by the observing system. Therefore, the deviation of the phase change is small, and it can be assumed to be single valued for every image point. For this optical imaging system there is a one-to-one correspondence between

Contrails

points on the object, points on the localized fringe pattern, and corresponding points on the two image planes, the image of the object and the image of the fringe pattern. From this procedure and with previous knowledge of a point on the object with zero displacement (or location of a zeroth-order fringe), the components of displacements parallel to the vector $\bar{k}_1 - \bar{k}_2$ can be determined for each object point.

Since the hologram has recorded a larger bundle of rays from each object point, the observing optical system can be moved parallel to the hologram so as to select a different ray from each object point and a different basis vector, $\bar{k}_1 - \bar{k}_2$. If this procedure is repeated again, three basis vectors can be obtained and the scalar components of displacement for each point on the object can be measured. The angular separation between any two of these basis vectors is limited by the hologram aperture. In this practice, this means that the angular separation will be small, and the sensitivity will be significantly less for measuring in-plane displacement components than for components normal to the hologram.

To obtain maximum sensitivity of the in-plane components using the above method the entire aperture of the hologram should be used. That is, the three basis vectors would be selected using three observations through the outer edges of the hologram aperture. Three photographs would be taken, and three fringe order numbers would be assigned to each object point. To obtain the in-plane components, a transformation of coordinates would have to be undertaken.

Other methods for measuring the in-plane components have been developed (Ref. 5, 6, 7), all of which are equivalent in concept to the above method in that they make use of localized fringes and that the measurement sensitivity is limited by the hologram aperture. Measurement of in-plane components using localized fringes was first accomplished (Ref. 5) by counting the number of fringes passing an object point as the observer moves his perspective. Although this can be accomplished only on a point-to-point basis, a refinement of this technique would be to move a camera lens laterally through a known angle and record two photographs while noting the direction and the number of fringes shifted. Another technique makes use of a rectangular slit of variable width (Ref. 6) which can be rotated to obtain maximum fringe contrast. Still another technique makes use of a cylindrical lens (Ref. 7) to measure the in-plane component on a point-to-point basis. These latter methods may be more convenient to measure in-plane components on a point-to-point basis; however, for purposes of displaying the entire field of in-plane components these techniques would have to be upgraded significantly to include perhaps some type of sophisticated scanning technique.

3. Accuracy and Minimum Detectability of In-Plane and Normal Components

The measurement accuracy and minimum detectable limit of the in-plane component are much less than the normal component because measurement of the in-plane component depends directly on the hologram aperture. The following paragraphs present a comparison of the accuracy and minimum detectable limit for the in-plane and normal components.

Contrails

a. Accuracy and Minimum Detectable Limit of the Normal Component

For static displacements, double exposure hologram, the normal component at the position of the n th order dark fringe is given by:

$$L_n = \frac{2n-1}{4} \lambda \quad (4)$$

where n is a positive integer and an obliquity factor of 2 is assumed. The uncertainty in the normal component depends upon the uncertainty in the obliquity factor and the uncertainty of locating the center of the n th dark fringe. The position of a dark band can be measured to within 10% of the fringe spacing using a photograph and visual observation and to within approximately 1% of the fringe spacing using a microdensitometer (Ref. 8). If the obliquity factor is known exactly then the uncertainty in the normal component is:

$$\delta L_n = C \frac{\lambda}{2} \quad (5)$$

where C is 0.1 for visual observation and 0.01 using a microdensitometer. Using a helium-neon laser the uncertainty is 1.25 microinches for visual observation or 0.125 microinches using a microdensitometer.

To measure small displacements there must be at least one point on the object whose normal component is large enough to cause a first order dark band so that a reference percentage modulation can be established. Then the minimum detectable normal component would be one-fourth of the wavelength of light, or 6.23 microinches for visual observation. If the first dark band is observable, then under carefully controlled experimental

conditions the minimum detectable limit may be reduced by perhaps a factor of 10 using a microdensitometer. This would be accomplished by measuring the relative fringe contrast.

b. Accuracy and Minimum Detectable Limit of the In-Plane Component

Using Equation 3 for two different observations the in-plane component is

$$L_{\parallel} = (n_2 - n_1) \frac{\lambda}{|\bar{e}_{o_1} - \bar{e}_{o_2}|} \quad (6)$$

where $(n_2 - n_1)$ is the number of dark bands passing across the object point when the observation is changed from along the unit vector \bar{e}_{o_1} to along the unit vector \bar{e}_{o_2} . The uncertainty of the in-plane component depends on the uncertainty of locating the center of two dark fringes, which is no more than twice the uncertainty in locating the center of one. Therefore, the uncertainty of the in-plane component is:

$$\delta L_{\parallel} = \frac{C \lambda}{|\bar{e}_{o_1} - \bar{e}_{o_2}|} \quad (7)$$

where C is 0.2 for visual observation and 0.02 with a microdensitometer. The absolute value of the vector in the denominator is directly proportional to the angle subtended by the usable aperture of the hologram and, for most practical cases, is much less than unity. For a four-by-five inch hologram, located 35 inches from the object where the effective aperture is 3.5 inches, the denominator of Equation 7 is approximately 0.1. Under these conditions the uncertainty in the in-plane component (using a helium-neon laser) is 50 microinches for visual observation and 5.0 microinches with a

microdensitometer. Some improvement in these figures may be obtained along the 5 inch dimension of the hologram or for larger holograms.

Figure 1 shows a plot of the error in the in-plane component as a function of the hologram to object distance assuming that the maximum useable aperture of the hologram is 3.5 inches.

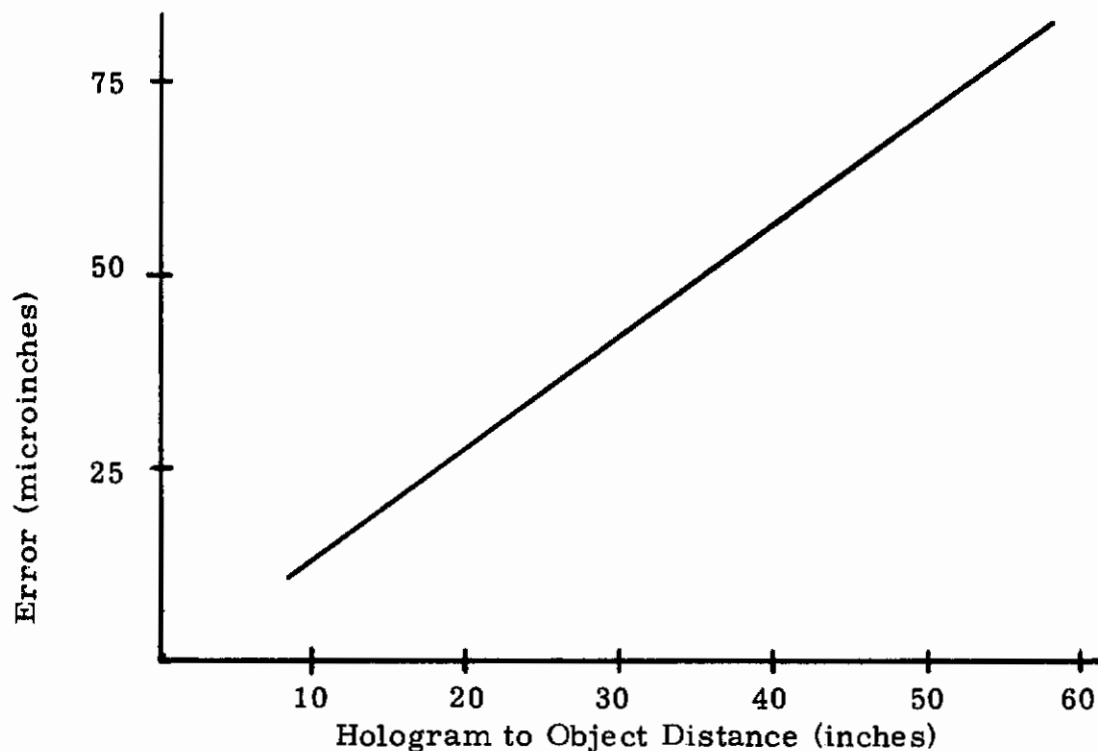


Figure 1. Error in the In-Plane Component Assuming Visual Observation and a Hologram Aperture of 3.5-inches

To measure small in-plane displacements there must be an observable dark and bright band so that a reference percentage modulation can be established. Then, at best, the minimum detectable fringe shift would be from a dark band to a bright band for visual observation. Under

carefully controlled experimental conditions, using a microdensitometer, a fringe shift as small as one-tenth of the distance between consecutive dark bands can be detected. For a useable hologram aperture of 3.5 inches located 35 inches from the object the minimum detectable in-plane component would be 125 microinches for visual observation and 25 microinches using a microdensitometer. Figure 2 is a plot of the minimum detectable in-plane component as a function of the hologram to object distance assuming a useable hologram aperture of 3.5 inches.

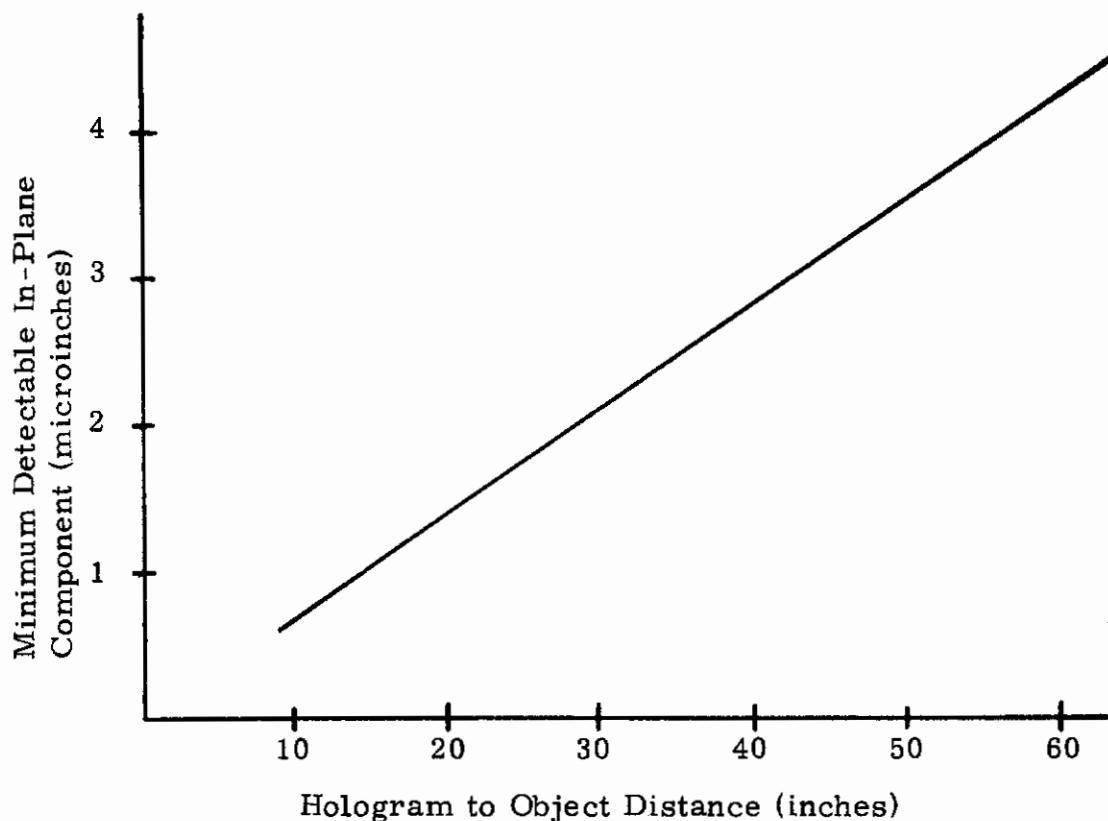


Figure 2. Minimum Detectable In-Plane Component Assuming Visual Observation and a Hologram Aperture of 3.5 Inches.

c. Summary

The accuracy of measuring displacements in holographic interferometry depends on the uncertainty of locating the center of a particular dark band. Measurement of minimum detectable normal and in-plane components requires an observable bright and dark band so that a reference percentage modulation can be established. Both the error and the minimum detectability of the in-plane are significantly higher than the normal component if the angle subtended by the hologram with the object is small. Table 1 shows a comparison of the error and minimum detectability between the in-plane and normal components for a usable hologram aperture of 3.5 inches located 35 inches from the object.

Table 1. Comparison Between In-Plane and Normal Components Assuming a 3.5-Inch Aperture Located 35 Inches from the Object.

	Normal Component		In-Plane Component	
	Micro-meters	Micro-inches	Micro-meters	Micro-inches
Error				
Visual	0.032	1.24	1.27	50
Microdensitometer	0.003	0.12	0.127	5.0
Minimum Detectable Component				
Visual	0.16	6.2	3.16	125
Microdensitometer	0.016	0.62	0.63	25

SECTION III

MEASUREMENT OF IN-PLANE DISPLACEMENTS USING LARGE APERTURE OBSERVATION

The experiment described in this section is a technique for directly measuring the in-plane component. The technique has good potential of being developed into a complete hardware system which will automatically measure and record entire displacement fields on magnetic tape. The technique, as developed in this study, is based on the collection of the entire reflected wave which is diffracted and recorded by the hologram from a single object point. In this way the entire fringe shift across the hologram aperture is recorded, from which the in-plane component can be computed.

1. Description of Technique

We are interested in the scalar phase change, due to the diffracted waves from a single object point in its original and displaced positions, as a function of the coordinates in the plane of the observing aperture. Referring to the coordinate system shown in Figure 3, the scalar phase change as a function of the unprimed coordinate system is given by:

$$\Omega = \frac{2\pi}{\lambda} \left[\bar{L} \cdot \bar{e}_i - \bar{L} \cdot \left(\hat{i} \frac{x}{R} + \hat{j} \frac{y}{R} + \hat{k} \frac{z}{R} \right) \right] \quad (8)$$

where the vector in parenthesis is the unit observation vector as a function of the coordinates of the point P in the plane of the observing aperture and R is the distance from the object point to the point P. If the phase change as given by Equation 8 varies sufficiently across the aperture, then an interference pattern can be observed, provided that the corresponding interference patterns from the remaining object points can be eliminated

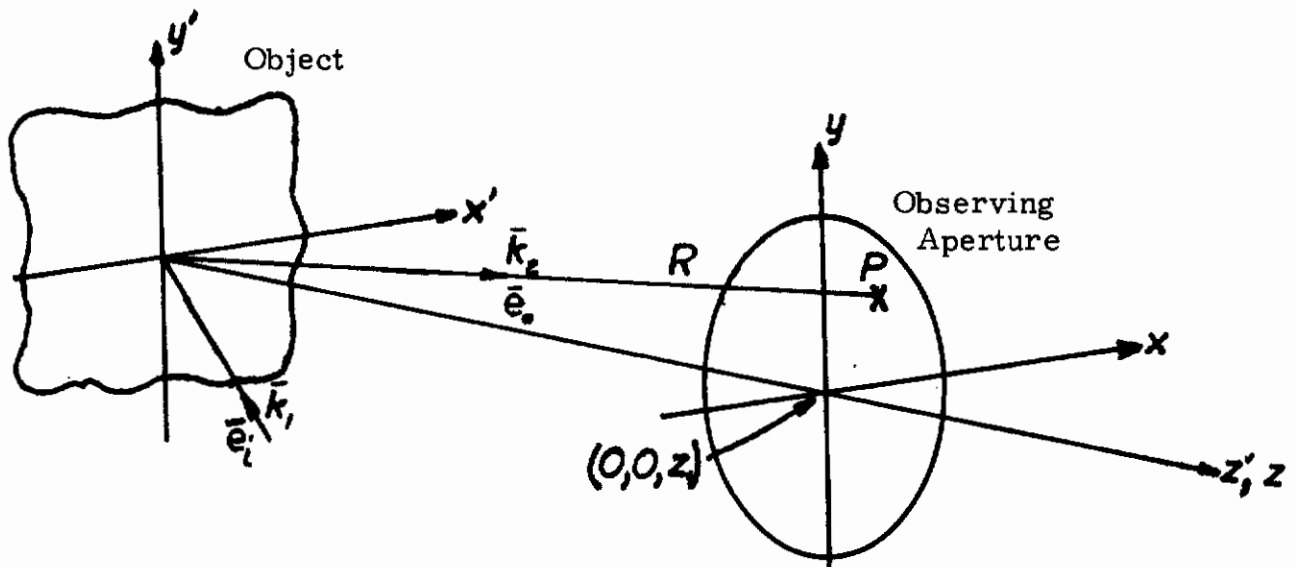


Figure 3. Coordinate System for Observing the Diffracted Waves from an Object Point

from the viewer. In practice, this can be accomplished by the experimental system shown in Figure 4. The first lens is as large as the hologram aperture and collects all of the wave diffracted from the object point that was recorded on the hologram. The pinhole filter is placed in the image plane of the object and selects only the single object point Q . Lens 2 collects the filtered interference pattern and images it onto the film plane.

Suppose that the displacement vector of the point Q is along the x -axis then Equation 8 becomes:

$$\Omega = \frac{2\pi}{\lambda} \left(\bar{\epsilon}_i \cdot \hat{\Gamma} L_x - \frac{x}{R} L_x \right) \quad (9)$$

where L_x is the magnitude of the displacement. The first term in Equation 9 is a constant phase term across the aperture. For static displacements, the dark bands will be given by values of x for which the phase change is

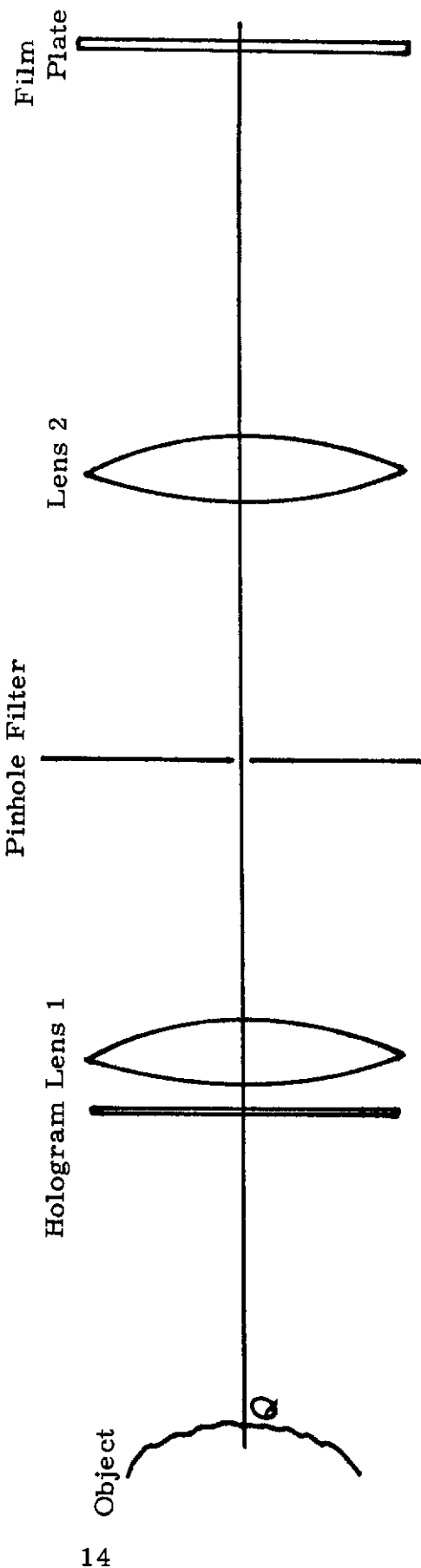


Figure 4. Optical System for Recording Fringe Shift Across Hologram Aperture

Contrails

an odd multiple of π . Therefore, the first term in Equation 9 will alter the position of the dark bands on the observing aperture, but not their spacing or their total number across the aperture. If the aperture is small compared to its distance from the object, then R is independent of x and y, and the fringes will be parallel to the y-axis. The direction of the in-plane displacement is perpendicular to the fringes, and its magnitude is given by:

$$L_x = \frac{R}{\Delta x} \lambda \quad (10)$$

where Δx is the fringe spacing and R is the object to aperture distance.

2. Experimental Results

To obtain a known in-plane displacement an optical translating mount was fastened into a holographic recording system similar to that shown in Figure 5. The translating stage was mounted parallel to the hologram and driven by a Lansing, Model 22.501, Differential Screw Micrometer. This micrometer is calibrated in dimensions of 10 microinches.

The optical stage was translated 300 microinches and a double-exposure hologram was recorded. Figure 6 is a photograph of the hologram image of the translating stage, and Figure 7 is a photograph of the hologram image of the fringes. The fringes were found to localize several inches behind the object. This is due to the fact that the illuminating wave was spherical rather than plane (Ref. 3).

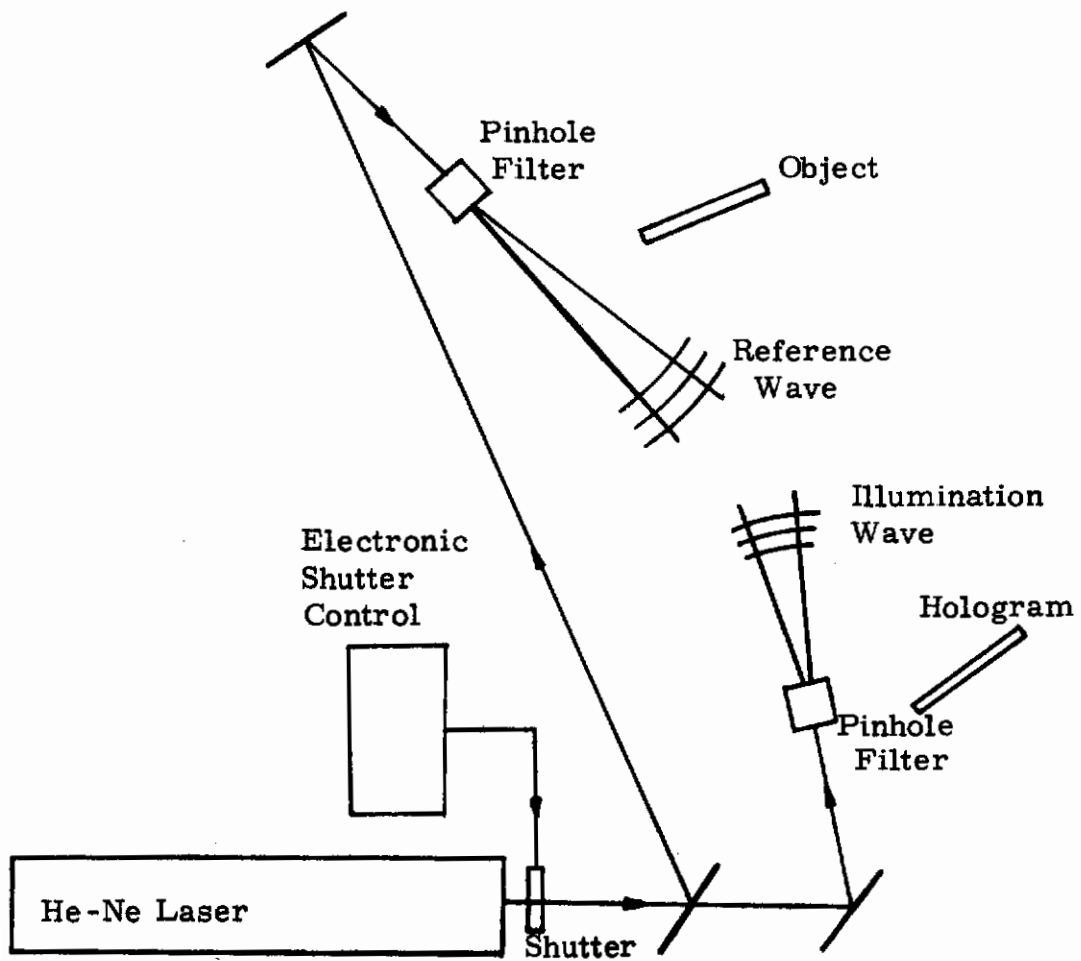


Figure 5. System for Recording and Viewing Hologram

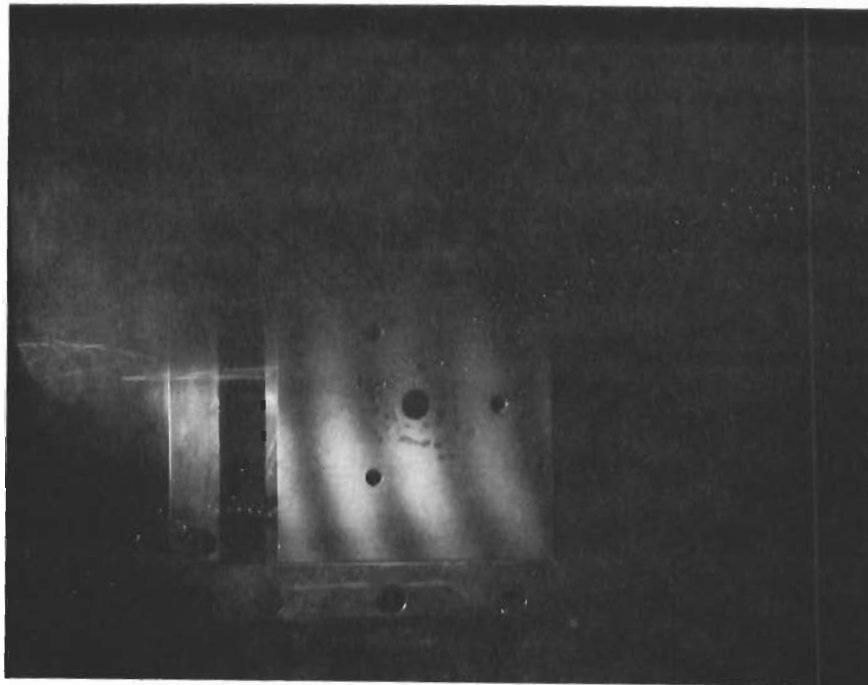


Figure 6. Photograph of Image of the Translating Stage

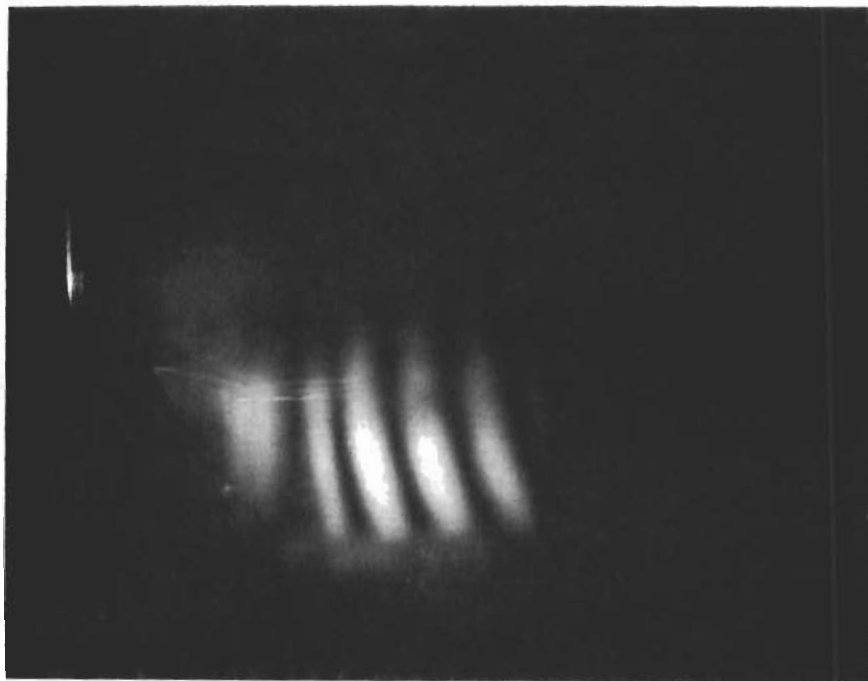


Figure 7. Photograph of Hologram Image of the Fringes

Contrails

The hologram was set up in the large aperture system shown in Figure 4. An object point in the center of the translating stage was selected by a 9/64-Inch diameter pinhole filter. The diameter of lens 1 was 4 inches. The resulting fringe pattern was recorded on polaroid film and is shown in Figure 8. Figure 9 is a photograph of the same object point except a 2.75-Inch aperture was placed directly in front of lens 1. Notice that the number of fringes is reduced but their fringe spacing remains the same. Also, the pinhole was moved laterally in order to select other object points, and as expected the fringe pattern remained the same indicating that other points on the stage have the same in-plane displacement.

The in-plane displacement can be computed from the fringe patterns and Equation 10. The distance from the object to lens 1 was 15.6 inches. The fringe spacing can be determined by computing the ratio of the fringe spacing to the total fringe field and multiplying this ratio by 4 inches and 2.75 inches for the fringe patterns of Figures 8 and 9 respectively. Following this procedure and using Equation 10, in-plane displacements of 287 and 330 microinches were obtained from Figure 8 and 307 microinches were obtained from Figure 9. Comparing these results with that read directly from micrometer, yields differences of 4.3%, 10%, and 2.3%, respectively.

The smallest difference was obtained when the 2 3/4-Inch aperture was placed in front of lens 1. This is probably due to the off-axis aberration introduced when the full aperture of lens 1 is utilized. This source of

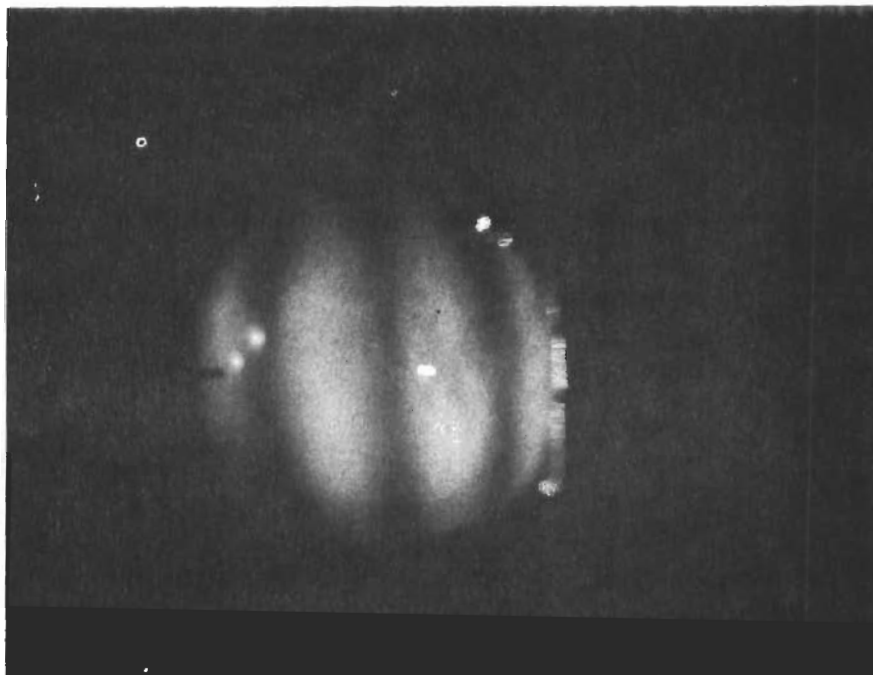


Figure 8. Fringe Pattern from Single Object Point (4" Aperture)

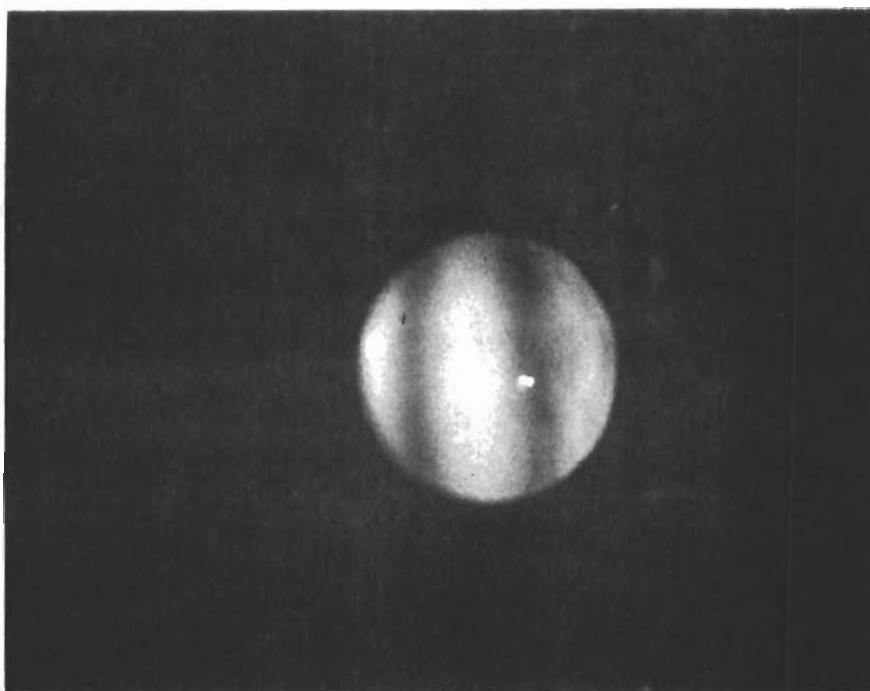


Figure 9. Fringe Pattern from Single Object Point (2 3/4" Aperture)

error could be reduced substantially in a completely developed system with the use of improved optics and suitable calibration procedures.

The differences between these measurements are consistent with the predicted error of the in-plane component shown in Figure 1 for a 3.5-Inch aperture located 15.6 inches from the object.

As additional information, the fringes viewed through the hologram in the usual manner (Figures 6 and 7) are caused by the variation of the vector $\bar{k}_2 - \bar{k}_1$ in Equation 3. This suggests a method of measuring whole-body translations directly from the fringe spacing.

3. Summary

A technique for measuring the in-plane component has been proposed. The technique has good potential of being developed into a complete hardware system which will automatically measure and record entire displacement fields on magnetic tape. The accuracy and minimum detectable component which can be measured by this technique are limited by the hologram aperture as given in Figures 1 and 2.

SUMMARY AND RECOMMENDATIONS

The technique described in this report when combined with a suitable technique for measuring the normal component could be developed into a complete hardware system for automatically measuring and recording displacement fields on magnetic tape. An inherent disadvantage in such a system is the somewhat larger error and decreased sensitivity of the in-plane component when a single hologram approach such as this is used. Although this approach or some modification of it may find ultimate use in an automatic system, it is believed that further work should be undertaken to improve the measurement capability of the in-plane component. This basically must involve measuring components along basis vectors whose angular separation are much larger. Such methods may involve the use of mirrors to observe the object through the same hologram from more oblique angles or the use of two or more illumination beams and dividing up the hologram into smaller holograms for each illumination beam.

Double exposure speckle photography using two oblique beams is an inherently more accurate technique for measuring the in-plane component. The advantages and disadvantages of two-illumination beam holography and two-beam speckle photography should be investigated with regard to accuracy, sensitivity, and testing convenience.

REFERENCES

1. K. A. Stetson, *Optik* 29 (1969), 386-400.
2. G. M. Brown, R. M. Grant, and G. W. Stroke, *J Acoustical Soc of Amer* 45 (1969), No. 5, pp 1166-1179.
3. Nils-Erik Molin and K. A. Stetson, *Optik* 31 (1970), pp 157-177 and pp 281-291.
4. K. A. Stetson, *Optik* 31 (1970), No 6, pp 576-591.
5. E. B. Aleksandrov and A. M. Bonch-Bruevich, *Soviet Physics - Technical Physics* 12, No 2 (Aug 1967), pp 258-265.
6. C. H. F. Velzel, *J Opt Soc of Amer*, 60, No. 3, (March 1970), 419-420.
7. C. Alpin, B. Marrone, and C. Minard, Laboratoires de Marcoussis, Marcoussis, France, "A New Holographic Fringe Analysis Technique".
8. "Vibration, Flutter, and Transient Analysis using Holographic Methods" Final Report, Contract NAS8-21369, June 1970 (N71-18982).

UNCLASSIFIED

Security Classification

DOCUMENT CONTROL DATA - R & D		
<i>(Security classification of title, body of abstract and indexing annotation must be entered when the overall report is classified)</i>		
1. ORIGINATING ACTIVITY (Corporate author) Air Force Flight Dynamics Laboratory Wright-Patterson Air Force Base, Ohio 45433		2a. REPORT SECURITY CLASSIFICATION UNCLASSIFIED 2b. GROUP
3. REPORT TITLE A TECHNIQUE FOR MEASURING IN-PLANE DISPLACEMENTS BY HOLOGRAPHIC INTERFEROMETRY		
4. DESCRIPTIVE NOTES (Type of report and inclusive dates) January 1971 to September 1971		
5. AUTHOR(S) (First name, middle initial, last name) Frank D. Adams, Richard R. Corwin		
6. REPORT DATE February 1972	7a. TOTAL NO. OF PAGES 22	7b. NO. OF REFS 8
8a. CONTRACT OR GRANT NO.	9a. ORIGINATOR'S REPORT NUMBER(S) AFFDL-TR-72-5	
b. PROJECT NO. 1467 c. Task No. 146702 d.	9b. OTHER REPORT NO(S) (Any other numbers that may be assigned this report)	
10. DISTRIBUTION STATEMENT Approved for public release, distribution unlimited.		
11. SUPPLEMENTARY NOTES	12. SPONSORING MILITARY ACTIVITY Air Force Flight Dynamics Laboratory AFFDL/FBR Air Force Systems Command Wright-Patterson Air Force Base, Ohio 45433	
13. ABSTRACT An experimental technique for measuring in-plane displacements from a single hologram is described. The method is based upon imaging the entire wave reflected from a single point and recorded on a hologram. Experimental results are presented. Application and limitations of the technique are discussed.		

DD FORM 1473
1 NOV 65

UNCLASSIFIED

Security Classification

UNCLASSIFIED

Security Classification

14. KEY WORDS	LINK A		LINK B		LINK C	
	ROLE	WT	ROLE	WT	ROLE	WT
Holographic interferometry						
Holography						
Metrology						
Experimental stress analysis						
Laser applications						

UNCLASSIFIED

Security Classification